The HKU Scholars Hub   The University of Hong Kong   香港大學學術庫

Title	On the timing behaviour of PSR B1259–63 under the propeller torque from a transient accretion disc
Author(s)	Yi, S; Cheng, KS
Citation	Monthly Notices of the Royal Astronomical Society, 2018, v. 476 n. 1, p. 766-770
Issued Date	2018
URL	http://hdl.handle.net/10722/253481
Rights	Monthly Notices of the Royal Astronomical Society. Copyright © Oxford University press, co-published with Royal Astronomical Society.; This article has been accepted for publication in [Monthly Notices of the Royal Astronomical Society] ©: [2018] [owner as specified on the article] Published by Oxford University Press on behalf of the Royal Astronomical Society. All rights reserved.; This work is licensed under a Creative Commons Attribution-NonCommercial-NoDerivatives 4.0 International License.

On the timing behaviour of PSR B1259–63 under the propeller torque from a transient accretion disc

Shu-Xu Yi[*] and K. S. Cheng[*]

Department of Physics, University of Hong Kong, Pokfulam Road, Hong Kong

ABSTRACT

The γ-ray pulsar binary system PSR B1259–63 flares in GeV after each periastron. The origin of these flares is still under debate. Recently, in 2017, we proposed a mechanism that might explain the GeV flares. In that model, a transient accretion disc is expected to be formed from the matter that was gravity-captured by the neutron star from the main-sequence companion's circumstellar disc. The transient accretion disc exerts a spin-down torque on the neutron star (i.e. the propeller effect), which might be traceable via pulsar timing observations of PSR B1259–63. In this paper, we consider the propeller effect phenomenologically using a parameter χ, which describes the coupling between the disc matter and the neutron star. Comparing the expected timing residuals with recent observations by Shannon et al., we conclude that the angular momentum transfer is very weak (with the coupling parameter $\chi \leq 10^{-4}$).

Key words: binaries: close – stars: emission-line, Be – pulsars: individual: PSR B1259–63 – gamma rays: stars.

1 INTRODUCTION

PSR B1259–63/LS2883 is a close binary system, which is composed of a millisecond pulsar (PSR B1259-63) and a massive Be star (LS2883). The Be star rotates rapidly and develops a decretion disc (circumstellar disc, CD) in its equatorial plane. Because the orbit of the pulsar is highly eccentric, with eccentricity $e = 0.87$, and because the closest distance between the pulsar and the Be star is very small, $\sim$0.9 au (Negueruela et al. 2011), the radio emission from the pulsar is eclipsed by the CD during $\sim T_0 \pm 15$ d (Johnston et al. 1996), where T_0 is the epoch of periastron. The interaction between the pulsar wind and the stellar wind (and/or the CD) gives rise to emission in X-ray and TeV bands (Hirayama et al. 1999; Kirk, Ball & Skjæraasen 1999; Aharonian et al. 2005; Chernyakova et al. 2006, 2014).

The binary has also been found to be a GeV source, by the *Fermi* satellite (Abdo et al. 2011; Tam et al. 2011). The GeV emission is puzzling: it remains quiescent through the orbit before a sudden flare at $\sim T_0 + 30$ d, where the pulsar is far away from the CD, and then gradually fades away in the following $\sim$15 d. The mechanism of the GeV emission is still under debate (Khangulyan et al. 2012; Kong, Cheng & Huang 2012; Dubus & Cerutti 2013; Mochol & Kirk 2013). With multiwavelength observations of the system around the 2014 periastron passage, Chernyakova et al. (2015) found that the onset of the GeV flare coincided with the

rapid decay of the H α equivalent width, which favours the model proposed by Chernyakova et al. (2014). Recently, we proposed a new model to account for the GeV flare of this system (Yi & Cheng 2017, hereafter Y17). In that model, matter from the CD is transferred to the gravity-capture radius of PSR B1259–63 and a transient accretion disc is developed around the neutron star.

If the transient accretion disc does appear in each orbit, then we shall expect the transfer of angular momenta between the accretion disc and the neutron star. In cases where the Keplerian velocity at the inner edge of the accretion disc is less than the corotating velocity with the neutron star, the accreted matter is stopped and ejected by the centrifugal force. This is known as the propeller effect (Illarionov & Sunyaev 1975). As a result, the pulsar experiences a spin-down torque. We introduce the propeller torque in the next section.

Timing observations of PSR B1259–63 are a natural way to study the potential time-varying braking torque from the transient disc. Manchester et al. (1995) found that the timing data of this pulsar can only be fitted after a jump of spin frequency is included in the model of spin evolution (also known as the timing solution) at each periastron. They suggested that it was a clue to the propeller spin-down. Wex (1998) found a timing solution different from that of Manchester et al. (1995), by including derivatives of the longitude of periastron passage (ω) and the projected pulsar semimajor axis (x). Those derivatives originate from the quadrupole gravitational moment of the Be star (Lai, Bildsten & Kaspi 1995). Wang, Johnston & Manchester (2004) applied three different timing solutions to the pulse times of arrival (TOAs) of PSR B1259–63: (i) with $\dot{\omega}$ and

[*] E-mail: yishuxu@hku.hk (S-XY); hrspksc@hku.hk (KSC)

$\dot{x}$ included; (ii) with jumps of the spin frequency and of its first derivative included at each periastron ($\Delta\nu$ and $\Delta\dot{\nu}$); (iii) with jumps of x at each periastron included (δx). Solutions (ii) and (iii) result in significantly smaller root-mean-square (rms) values in the timing residuals than solution (i), and solution (iii) was preferred because it had fewer degrees of freedom. Using a more sophisticated orbit–spin coupling model, Shannon, Johnston & Manchester (2014, hereafter S14) fitted the TOAs such that the residuals showed no orbital modulated timing residuals.

Because the timing solution of S14 fits the TOAs of PSR B1259–63 so well without requiring additional orbital modulated braking torques, their work can be used to set a limit on the transient disc scenario. In other words, if the propeller effect of the transient accretion disc is significant enough, then any timing solution that does not consider it cannot fit the TOAs so well. In this paper, we study the timing residuals of the pulsar that result if the transient disc proposed in Y17 does appear around the pulsar after each periastron. Under the constraint from S14, the Y17 scenario is strongly limited.

2 BRAKING TORQUE FROM THE PROPELLER EFFECT

The spin-down rate of a pulsar that undergoes the propeller effect is composed of two parts,

$$\dot{\nu} = \dot{\nu}_{\text{prop}} + \dot{\nu}_{\text{dip}}, \tag{1}$$

where $\dot{\nu}_{\text{prop}}$ is a result of the propeller effect and $\dot{\nu}_{\text{dip}}$ is a result of the magnetic dipole radiation. The spin-down torque exerted by the accretion disc can be calculated directly using

$$N_{\text{prop}} = -\int_{r_{\text{M}}}^{\infty} r^2 B_\phi B_z \, dr, \tag{2}$$

both analytically (see Ghosh & Lamb 1979b, and references therein) or numerically (see Romanova et al. 2004, and references therein). Here, B_ϕ is the azimuthal magnetic field induced by the disc matter, B_z is the vertical magnetic field component that penetrates the disc and r_{M} is the inner edge of the accretion disc. Many other authors estimate the spin-down torque indirectly, by calculating the rate at which angular momentum is taken away by the ejected matter from the accretion disc (e.g. Menou et al. 1999; Liu et al. 2014):

$$2\pi I \dot{\nu}_{\text{prop}} = 2 r_{\text{M}}^2 \dot{M}_{\text{acc}} \left(\sqrt{\frac{GM_\star}{r_{\text{M}}^3}} - 2\pi\nu \right) \chi. \tag{3}$$

Here, I, ν, $M_\star$ and $\dot{M}_{\text{acc}}$ are the rotational inertia, the spin frequency, the mass of the pulsar and the accretion rate of the disc at the innermost radius, respectively; χ ($0 < \chi < 1$) is the coefficient describing the degree of coupling between the accretion disc and the pulsar via the magnetic field lines. The factor of 2 on the right-hand side of equation (3) comes from the fact that there are two nearly equal contributions of the torque: the angular momenta transferred at the inner edge of the disc and the angular momenta transferred from the accretion flow to the magnetic field beyond the inner edge (Menou et al. 1999).

The link between the two approaches gives $2\chi = \sqrt{2}\gamma_a\delta$ (Dai & Li 2006), where $\gamma_a \sim B_\phi/B_z$ and $\delta \ll 1$ is the ratio between the width of the boundary layer of accretion and the inner radius of the accretion disc (Ghosh & Lamb 1979a). Here, B_ϕ is generated by rotation shear. If the magnetosphere is nearly force-free, then the azimuthal pitch γ_a should be of the order of unity (see Aly & Kuijpers 1990; Livio & Pringle 1992). As a result, $\chi \ll 1$ is implied, which is in accordance with our findings below.
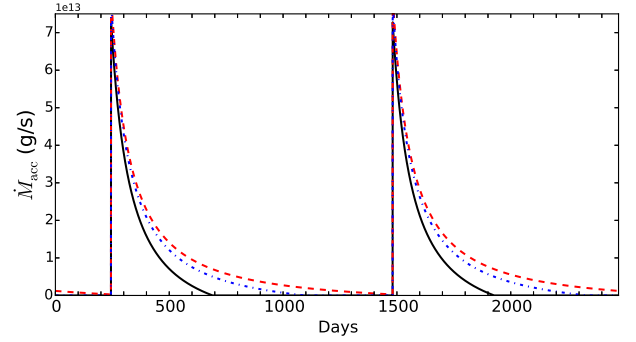
Figure 1. The accretion rate at $r = r_{\text{M}}$ when $\dot{M}_{\text{eva}} = 10^{13}$, 5×10^{12} and 3×10^{12} g s^{-1} (black solid, blue dash-dotted and red dashed curves, respectively). In order to illustrate the repetitive nature of the curves, we show two orbital periods.

In order to avoid dealing with the complexity and uncertainty of the magnetic field structure, we adopt equation (3) here. Note that r_{M} is supposed to be equal to the Alfvén radius, where the ram pressure of the accretion flow is balanced by the magnetic field pressure. Thus

$$r_{\text{M}} = 5.1 \times 10^8 \dot{M}_{\text{acc},16}^{-2/7} m_\star^{-1/7} \mu_{30}^{4/7} \text{ cm}, \tag{4}$$

where $\dot{M}_{\text{acc},16}$ is the accretion rate of the accretion disc in units of 10^{16} g s^{-1}, μ_{30} is the magnetic dipole in units of 10^{30} G cm^3 and $m_\star \equiv M_\star/M_\odot$.

If we assume that the accretion disc is the standard thin disc (Shakura & Sunyaev 1973), then

$$\rho = 3.1 \times 10^{-8} \alpha^{-7/10} \dot{M}_{\text{acc},16}^{11/20} m_\star^{5/8} R_{10}^{-15/8} \text{ g cm}^{-3}, \tag{5}$$

where α is the viscosity index and R_{10} is the radius in units of 10^{10} cm.

The scenario in which the transient disc is formed from gravity-captured materials is similar to the case where a fossil disc is formed from fall-back materials around a newly born neutron star. Therefore, we apply the equations from Chatterjee, Hernquist & Narayan (2000) to describe the evolution of the accretion rate at the inner edge of the disc:

$$\dot{M}_{\text{acc}} = \dot{M}_{\text{acc},0} - \dot{M}_{\text{eva}}, \qquad (r_{\text{in}} > r_{\text{M}});$$

$$\dot{M}_{\text{acc}} = \dot{M}_{\text{acc},0} \left(\frac{t}{\tau} \right)^{-\beta} - \dot{M}_{\text{eva}}, \qquad (r_{\text{in}} = r_{\text{M}}). \tag{6}$$

When $t = \tau$, the disc descends to r_{M}. Here, $\dot{M}_{\text{eva}}$ is the mass evaporating rate, which originates from γ-ray irradiation of the disc, as proposed by Takata, Cheng & Taam (2010), and it is chosen such that the accretion disc around the neutron star is cleaned before the formation of a new disc in the next orbit. Besides, we expect $\dot{M}_{\text{eva}}$ to be no larger than 10 per cent of $\dot{M}_{\text{acc},0}$ so that the validity of the mechanism of Y17 is not affected. The parameters of the model were found in our previous work by fitting the GeV light curve. For a Kramer disc opacity ($\beta = 1.25$), we found that $\dot{M}_{\text{acc},0} \approx 1 \times 10^{14}$ g s^{-1} and $\tau \approx 100$ d. (For a full description of the model and numerical values of other parameters, see Y17). The above restriction sets the range of $\dot{M}_{\text{eva}}$ to be from 3×10^{12} to 10^{13} g s^{-1}.

With the above parameters and equation (6), the accretion rate at r_{M} is calculated with different values of $\dot{M}_{\text{eva}}$ (10^{13}, 3×10^{12} and 5×10^{12} g s^{-1}). The accretion rate as a function of time is shown in Fig. 1, and it is repetitive with the orbital period of 1236.7 d. The accretion rate experiences a sudden increase and a slow decrease, the tail of which is determined by $\dot{M}_{\text{eva}}$. Note that when $t < \tau$, the
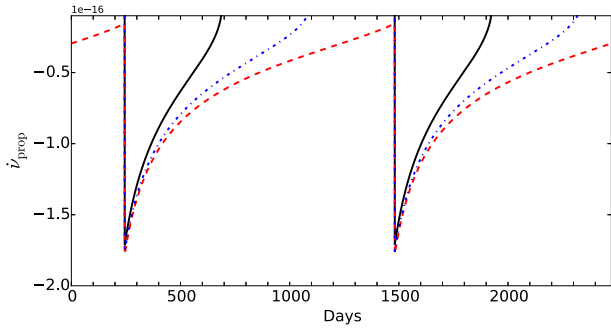
Figure 2. $\dot{\nu}_{prop}$ due to the propeller torque, when $\dot{M}_{eva} = 10^{13}$, 5×10^{12} and 3×10^{12} g s^{-1} (black solid, blue dash-dotted and red dashed curves, respectively), with the assumption that $\chi = 0.001$. In order to illustrate the repetitive nature of the curves, the horizontal span is two orbital periods.
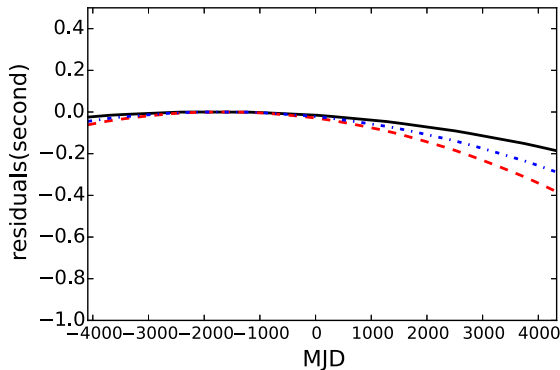
Figure 3. Additional timing residuals due to the braking torque from the propeller effect when $\dot{M}_{eva} = 10^{13}$, 5×10^{12} and 3×10^{12} g s^{-1} (black solid, blue dash-dotted and red dashed curves, respectively) and $\chi = 0.001$.

inner edge of the accretion disc has not yet descended to r_M. As a result, although the accretion rate at the inner edge is a constant $\dot{M}_{acc,0}$ as indicated in the first line of equation (6), the accretion rate at r_M is zero, as shown in Fig. 1.

Combining equations (3), (4) and (6), the values of $\dot{\nu}_{prop}$ are shown in Fig. 2. Note that $\dot{\nu}_{prop}$ as a function of time has an impulsive nature, which arises from the time dependence of the accretion rate.

## 3 RESULTANT TIMING RESIDUALS

As shown above, the transient accretion disc brings time-varying $\dot{\nu}_{prop}$ in addition to the previous spin evolution models. The corresponding changes to the spin frequency and the spin phase as functions of time are the first and second integrals of ν_{prop}, respectively. The resultant timing residuals (i.e. the difference between the theoretically modelled spin phases and the real spin phases divided by the spin frequency at a certain epoch) are

$$R(t) = \int_{t_0}^{t} \int_{t_0}^{t} \frac{\dot{\nu}_{prop}(t)\, \mathrm{d}t^2}{\nu_0}, \tag{7}$$

where t_0 is the epoch when the spin frequency of the pulsar equals ν_0. Fig. 3 shows the residuals as a function of MJD corresponding to different $\dot{M}_{eva}$.

Although previous spin evolution models do not include time-varying $\dot{\nu}_{prop}$, as a regular procedure they fit for a constant $\dot{\nu}$. This is equivalent to removing a parabolic structure from the spin phases as a function of time (see equation 7). As a result, the timing residuals plotted in Fig. 3 are largely reduced in the real observed residuals.
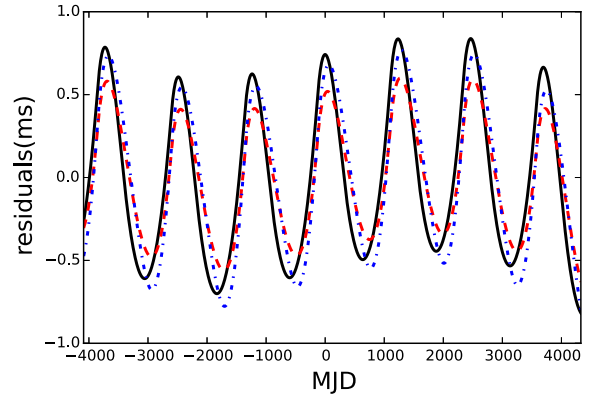
Figure 4. The timing residuals after fitting a constant $\dot{\nu}$ when $\dot{M}_{eva} = 10^{13}$, 5×10^{12} and 3×10^{12} g s^{-1} (black solid, blue dash-dotted and red dashed curves, respectively) and $\chi = 0.001$.
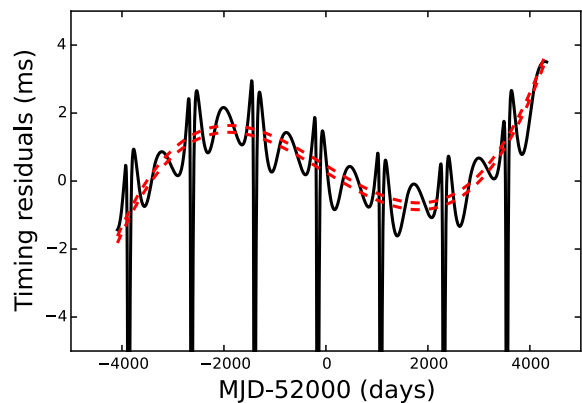
Figure 5. The timing residuals after all parameters are refitted when $\dot{M}_{eva} = 10^{13}$ g s^{-1} and $\chi = 10^{-3}$. The red dashed curves represent the upper and lower limits set by the TOA uncertainty and observed residuals.

Fig. 4 shows the residuals after fitting a constant $\dot{\nu}$. As we can see in Fig. 4, because of the fitting of a constant $\dot{\nu}$, the residuals are not sensitive to the choice of $\dot{M}_{eva}$ in the range from $\dot{M}_{eva} = 3 \times 10^{12}$ to $\dot{M}_{eva} = 10^{13}$ g s^{-1}. Thus, we take $\dot{M}_{eva} = 10^{13}$ g s^{-1} in the flowing calculation.

As we have shown above, the fitting of a constant $\dot{\nu}$ will absorb the most of the timing residuals. Similarly, the fitting of other parameters in the timing solution (e.g. the parameters of the binary orbit) will also reduce the timing residuals. We consider the absorption of timing residuals by fitting all the parameters in the timing solution of S14 in the following way. Using the software package TEMPO2 (Hobbs, Edwards & Manchester 2006), we generate a series of simulated TOAs using S14's timing solution, which corresponds to a weekly observation from MJD = 47910 to 56329. Then, we subtract the timing residuals calculated with equation (7) from the simulated TOAs, obtaining a new series of TOAs. All parameters in the timing model of S14 are set free to fit against the new TOAs, resulting in a series of timing residuals, as plotted in Fig. 5.

The spikes are residuals due to the Roemer delay of the highly eccentric orbit when the pulsar is around the periastron. If the propeller torque as described with equation (3) did present at each periastron with $\chi = 10^{-3}$, the structure shown in Fig. 5 should have been observed. Because the pulsar is eclipsed by the CD around the periastron, the days during these spikes are not included in the real observation data. In Fig. 5, the two red dashed curves are the
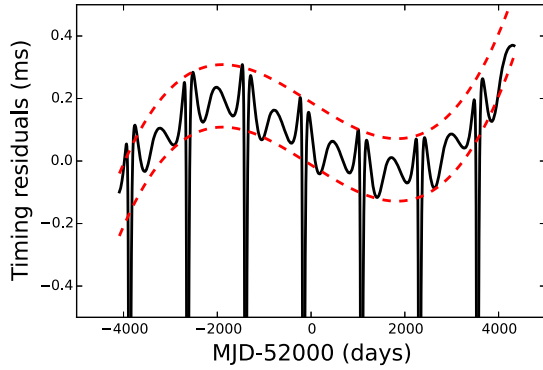
Figure 6. Same as in Fig. 5, but for $\chi = 10^{-4}$.

Figure 7. The absolute value of $\dot{\nu}_{prop}$ when $\chi = 10^{-4}$ (black dotted curves), the lower limit of $|\dot{\nu}_{prop}|$ set by inequality (8) (red solid curves) and $|\dot{\nu}_{prop}|$ set by equation (9) (blue dash-dotted curves).

upper and lower limits of the observed timing residuals, which are obtained by $\pm 100\,\mu$s from S14's timing residuals, as shown in their fig. 2 ($\pm 100\,\mu$s corresponds to the averaged TOA uncertainty). As shown in Fig. 5, the calculated timing residuals surpass those observed. Therefore, the propeller torque mechanism with $\chi = 10^{-3}$ is ruled out. We need a smaller value of χ so that the resultant timing residuals can agree with the observations.

With $\chi = 10^{-4}$, we repeat the procedures above. It is shown in Fig. 6 that the structure in the timing residuals remains in the range bounded by the TOA uncertainty. Thus, we set the limit that $\chi \leq 10^{-4}$.

4 DISCUSSION

As found above, the timing observation of PSR B1259–63 limits the coupling coefficient χ to be less than 10^{-4}. If we can somehow prove that this limitation is non-physical, then the Y17 mechanism confronts a great challenge. However, if there are justifications for why the coupling should be so small, then the Y17 mechanism can survive under the current test from timing observations.

The lower limit of the accretion spin-down can be set in the following way. It is natural to suppose that the propeller effect ejects the accreted matter at least with the escape velocity of the neutron star, or the matter will fall back. Therefore, the power of the propeller torque should be no less than the gravitational binding energy of the accreted matter per unit time. As a result,

$$2\pi|\dot{\nu}_{prop}| \geq \frac{|\dot{M}_{acc}(GM_\star/2r_M)|}{I\Omega_\star}. \tag{8}$$

Equation (8) corresponds to the argument that the energy transferred from the rotation of the pulsar in dt should be at least enough to eject mass dm from its bounded Keplerian orbit to an unbounded trajectory.

In Fig. 7, the lower limit of $|\dot{\nu}_{prop}|$ set by the equality (8) as a function of time is plotted (as the red solid curves), in comparison with $|\dot{\nu}_{prop}|$ calculated with equation (3) of $\chi = 10^{-4}$ (black dash-dotted curves). It can be seen that the limitation $\chi \leq 10^{-4}$ does not violate the lower limit set using equation (8).

Romanova et al. (2003) estimated the propeller torque theoretically using the following equation:

$$2\pi I \dot{\nu}_{prop} \approx -0.76\mu^{4/5} f^{2/5} \Omega^{3/5} \dot{M}^{3/5}. \tag{9}$$

Here, μ is the magnetic dipole of the neutron star and f is a factor for which the authors took $f = 0.3$. In Fig. 7, we plot $|\dot{\nu}_{prop}|$ calculated with equation (9) as blue dash-dotted curves. The numerical simulation of Romanova et al. (2003) showed that the torque was
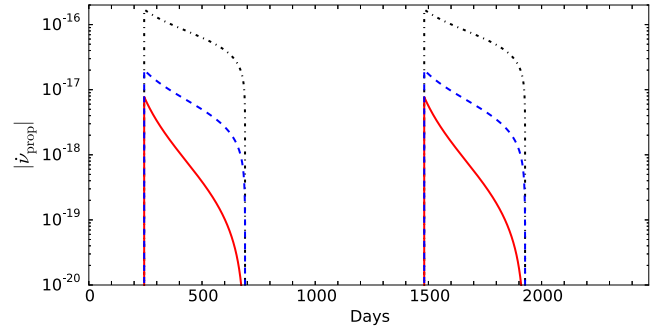
about 10 times larger than the value evaluated with equation (9), which is about the same as the value calculated with equation (3) with $\chi = 10^{-4}$ (red curves in Fig. 7). Although the simulation was made in the case of a spherical accretion, a later simulation of the accretion disc showed a similar result (Romanova et al. 2004).

The smallness of the propeller torque is understandable with equation (3). The extra spin-down torque arises from the bending of magnetic field lines, caused by disc matter, that penetrate the accretion disc. When the disc is in the wind zone, the poloidal magnetic field becomes radial asymptotically, and the toroidal component dominates (see the recent review by Cerutti & Beloborodov 2017). Therefore, there are fewer magnetic field lines that penetrate the disc. In the case of an aligned rotator and an infinitesimal thin disc outside the light cylinder, there is no magnetic field line going through the disc, and thus zero propeller torque is exerted by the disc.

5 SUMMARY

In order to explain the GeV flare of PSR B1259–63, Y17 proposed that a transient accretion disc is formed out of gravity-captured matter from the circumstellar disc of the Be star. We studied the timing behaviour of the pulsar, under the propeller torque from the proposed transient accretion disc phenomenologically. We conclude that no evidence of the propeller effect can be found in the recent timing observations of this system (S14). If the mechanism of Y17 were true, then the coupling parameter of propeller torque in equation (3) would be less than 10^{-4}.

REFERENCES

Abdo A. A. et al., 2011, ApJ, 736, L11
Aharonian F. et al., 2005, A&A, 442, 1
Aly J. J., Kuijpers J., 1990, A&A, 227, 473
Cerutti B., Beloborodov A. M., 2017, Space Science Reviews, 207, 111
Chatterjee P., Hernquist L., Narayan R., 2000, ApJ, 534, 373
Chernyakova M., Neronov A., Lutovinov A., Rodriguez J., Johnston S., 2006, MNRAS, 367, 1201
Chernyakova M. et al., 2014, MNRAS, 439, 432
Chernyakova M. et al., 2015, MNRAS, 454, 1358
Dai H-L., Li X-D., 2006, A&A, 451, 581

Dubus G., Cerutti B., 2013, A&A, 557, A127

Ghosh P., Lamb F. K., 1979a, ApJ, 232, 259

Ghosh P., Lamb F. K., 1979b, ApJ, 234, 296

Hirayama M., Cominsky L. R., Kaspi V. M., Nagase F., Tavani M., Kawai N., Grove J. E., 1999, ApJ, 521, 718

Hobbs G. B., Edwards R. T., Manchester R. N., 2006, MNRAS, 369, 655

Illarionov A. F., Sunyaev R. A., 1975, A&A, 39, 185

Johnston S., Manchester R. N., Lyne A. G., D'Amico N., Bailes M., Gaensler B. M., Nicastro L., 1996, MNRAS, 279, 1026

Khangulyan D., Aharonian F. A., Bogovalov S. V., Ribó M., 2012, ApJ, 752, L17

Kirk J. G., Ball L., Skjæraasen O., 1999, Astroparticle Physics, 10, 31

Kong S. W., Cheng K. S., Huang Y. F., 2012, ApJ, 753, 127

Lai D., Bildsten L., Kaspi V. M., 1995, ApJ, 452, 819

Liu X-W., Xu R-X., Qiao G-J., Han J-L., Tong H., 2014, Research in Astronomy and Astrophysics, 14, 85

Livio M., Pringle J. E., 1992, MNRAS, 259, 23p

Manchester R. N., Johnston S., Lyne A. G., D'Amico N., Bailes M., Nicastro L., 1995, ApJ, 445, L137

Menou K., Esin A. A., Narayan R., Garcia M. R., Lasota J.-P., McClintock J. E., 1999, ApJ, 520, 276

Mochol I., Kirk J. G., 2013, ApJ, 776, 40

Negueruela I., Ribó M., Herrero A., Lorenzo J., Khangulyan D., Aharonian F. A., 2011, ApJ, 732, L11

Romanova M. M., Toropina O. D., Toropin Y. M., Lovelace R. V. E., 2003, ApJ, 588, 400

Romanova M. M., Ustyugova G. V., Koldoba A. V., Lovelace R. V. E., 2004, ApJ, 616, L151

Shakura N. I., Sunyaev R. A., 1973, A&A, 24, 337

Shannon R. M., Johnston S., Manchester R. N., 2014, MNRAS, 437, 3255 (S14)

Takata J., Cheng K. S., Taam R. E., 2010, ApJ, 723, L68

Tam P. H. T., Huang R. H. H., Takata J., Hui C. Y., Kong A. K. H., Cheng K. S., 2011, ApJ, 736, L10

Wang N., Johnston S., Manchester R. N., 2004, MNRAS, 351, 599

Wex N., 1998, MNRAS, 298, 67

Yi S-X., Cheng K. S., 2017, ApJ, 844, 114 (Y17)

This paper has been typeset from a TEX/LATEX file prepared by the author.